Electron Inelastic Mean Free Paths in Liquid Water for Energies from10 eV to 10 keV.

S. Tanuma[1], H. Shinotsuka[1], B. Da[1], H. Yoshikawa[1], C. J. Powell[2]
[1]NIMS, Japan , [2]NIST, USA

1. Introduction
2. Calculations of IMFPs
3. Evaluations of ELF at q=0
4. Analysis of IMFPs
5. Comparisons with other calculations
6. Summary

1. Introduction

- important to know details of the interactions of low-energy electron with liquid water for many biological applications, especially for the investigation of cellular and sub-cellular dosimetry

- Inelastic mean free path (IMFP) : good measure most basic physical quantity

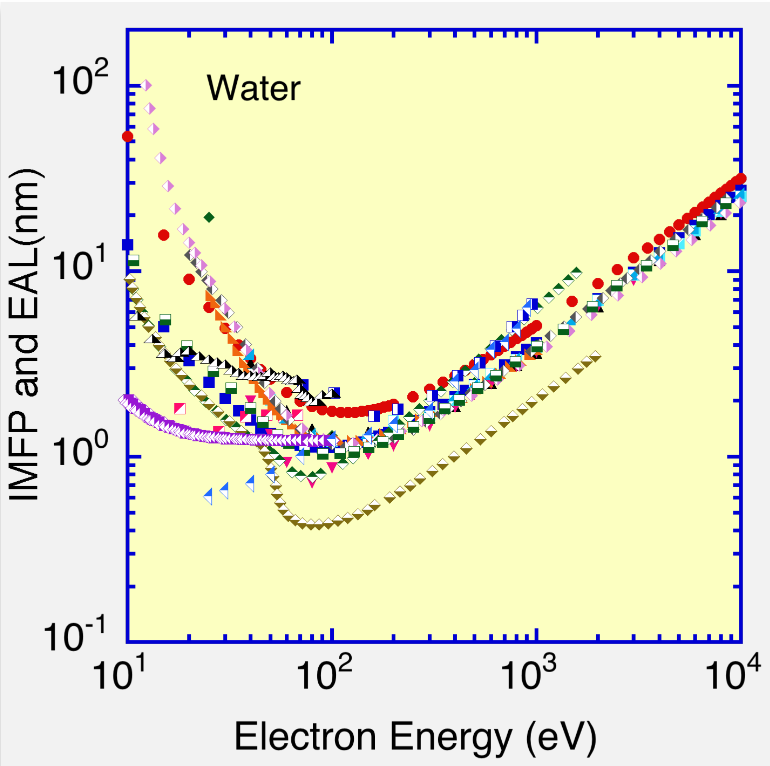

- many studies to determine the electron inelastic mean free paths (IMFPs) in water

- but large variations in IMFP values

- mainly due to the calculation algorithm and the energy-loss function (ELF) used for the IMFP calculations.

Calculation method of IMFP for water from ELF

:Relativistic inelastic DCS (< 0.5 MeV; Fernandez-Varea)

$$\frac{d^2\sigma}{d\omega dq} = \frac{2}{\pi N v^2} \mathrm{Im}\left(\frac{-1}{\varepsilon(q,\omega)}\right)\frac{1}{q}$$

$$n\sigma(T)\lambda(T) = 1$$

- ELF at q=0 can be measured
  - reflection method
  - X-ray inelastic scattering
  - EELS etc.
- estimation of ELF at q>0
  (very important)

: fit with Drude functions at q=0
  q- dependence
  - use dispersion equation
  ex. quadratic eq.
  quartic eq.

: direct use of numerical ELF at q=0
  q-dependence
  - Luindhard model ELF for q>0 (FPA)
  - single pole approximation (SPA) with quartic eq. for dispersion
  - SSPA with quadratic eq. for dispersion
  -

2. ELF(*q*,*ω*):FPA, SPA, SSPA

- FPA : Full Penn Algorithm

$$\mathrm{Im}\left[\frac{-1}{\varepsilon(q,\omega)}\right] = \int_0^\infty d\omega_p g(\omega_p)\,\mathrm{Im}\left[\frac{-1}{\varepsilon^L(q,\omega;\omega_p)}\right]$$

$$g(\omega) = \frac{2}{\pi\omega}\mathrm{Im}\left[\frac{-1}{\varepsilon(\omega,q=0)}\right]$$

- Use numerical ELF data at q=0 (without curve fit of; energy dependence)
- q-dependence (Lindhard model dielectric function)

- SPA :Single Pole Approximation or Simple Penn Approximation

$$\mathrm{Im}\left[\frac{-1}{\varepsilon(q,\omega)}\right] = \mathrm{Im}\left[\frac{-1}{\varepsilon(\omega_0)}\right] \Big/ \left\{1+\frac{\pi q^2}{6k_F(\omega_0)}\right\},$$

$$\omega_q^2(\omega_p) = \omega_p^2 + \frac{1}{3}\left(k_F(\omega_p)q\right)^2 + \frac{q^4}{4}$$

- quartic equation

- SSPA :Simplified SPA

$$\mathrm{Im}\left[\frac{-1}{\varepsilon(q,\omega)}\right] = \frac{\omega_0}{\omega}\mathrm{Im}\left[\frac{-1}{\varepsilon(\omega_0)}\right],$$

$$\omega_q(\omega_p) = \omega_p + \frac{q^2}{2}.$$

-quadratic equation

3. Evaluation of ELF(q=0) for water

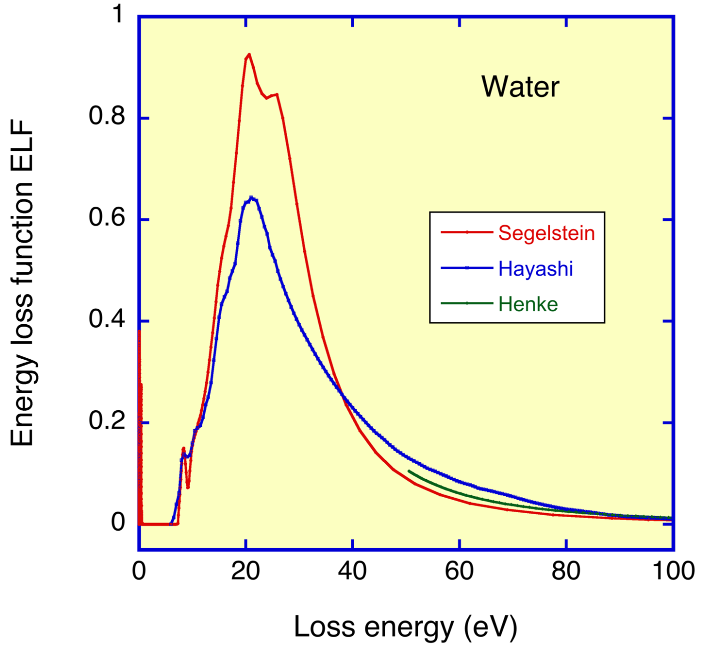

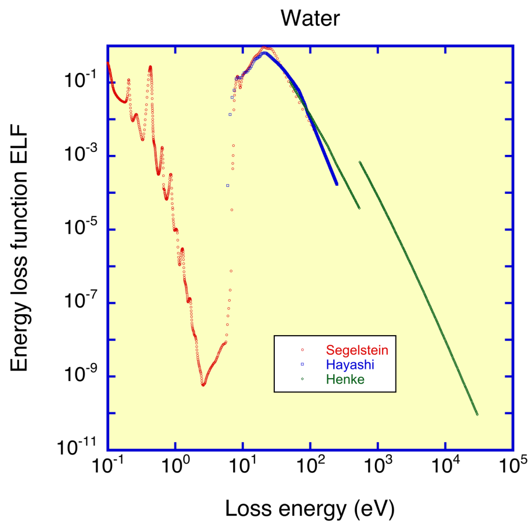

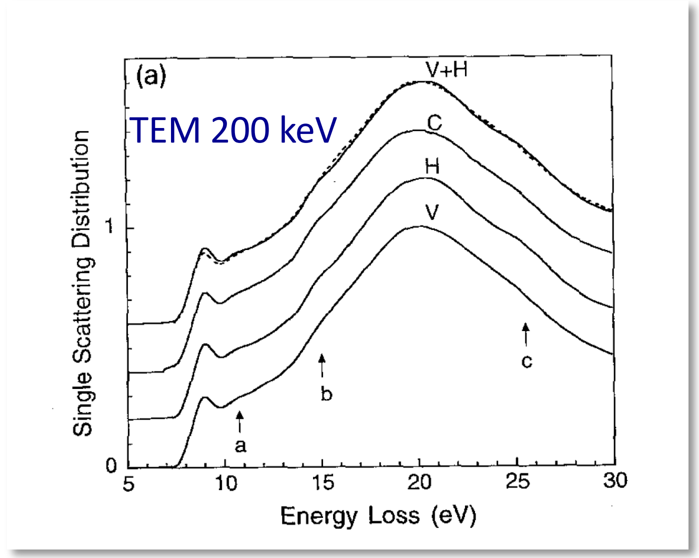

Model 1: <u>ELF #1</u>

- Seglestein + Henke

(1.24E-7 – 124 eV, 124eV- 30 keV)

Model 2: <u>ELF #2</u>

-Segelstein + Hayashi + Henke

(- 5.9 eV, 6- 87 eV, 87eV – 30 keV)

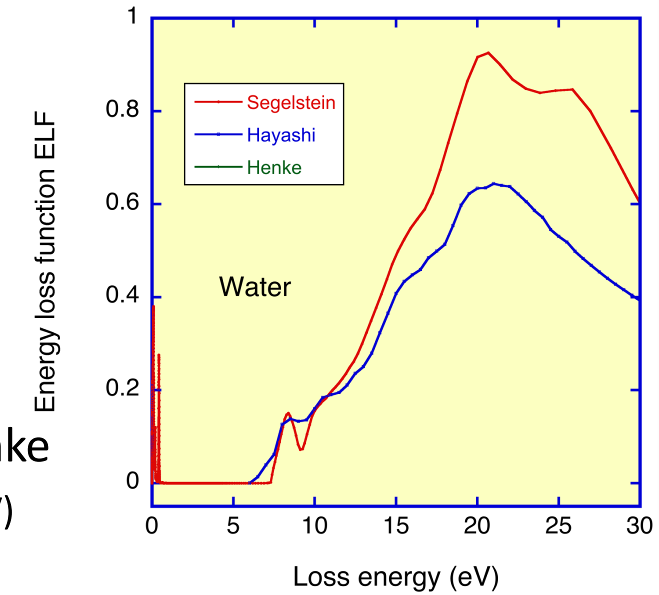

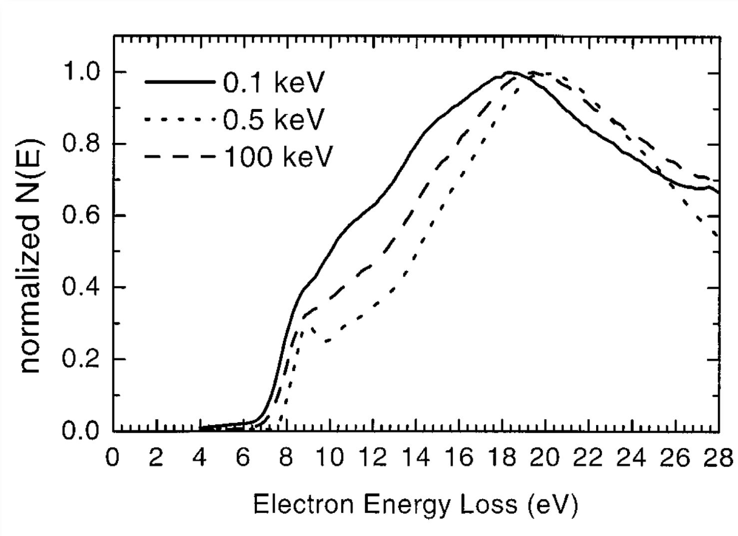

Evaluation of ELFs

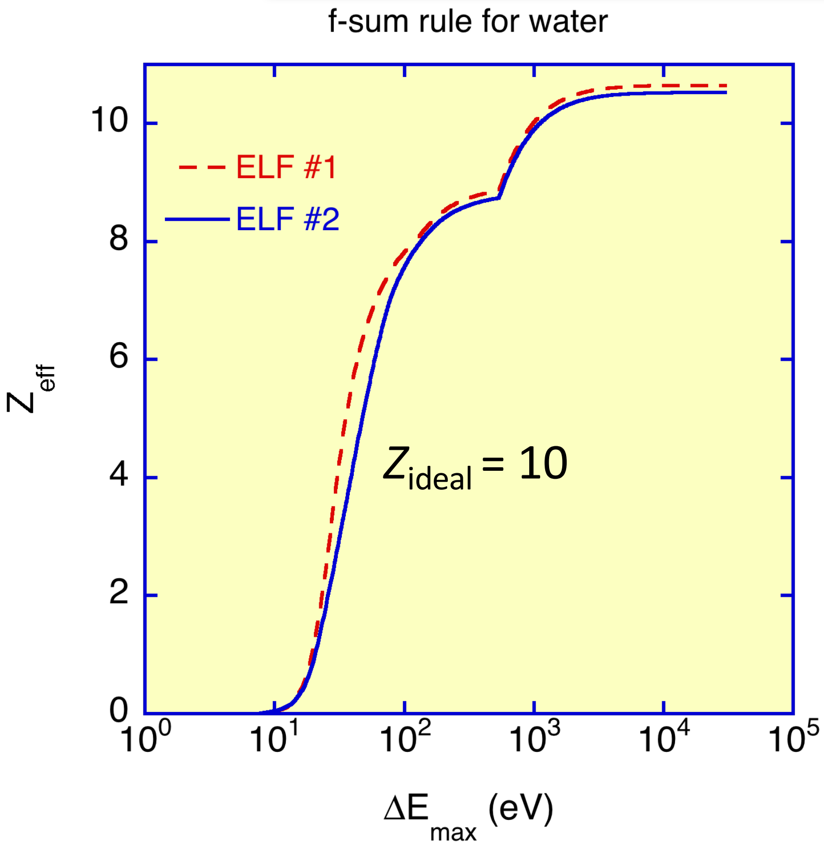

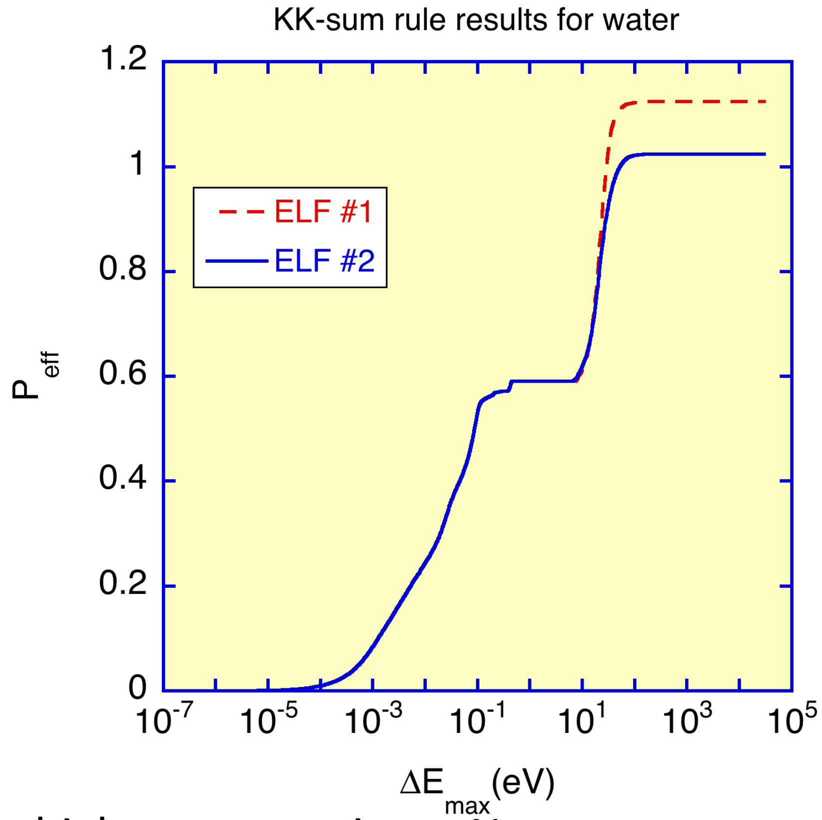

F-sum : evaluate ELF data at relatively high energy region – N_{eff}

results : ELF #1 10.6 ELF #2 10.5

KK-sum: evaluate ELF data at low energy region (theory = 1.0)

results: ELF #1 1.14 ELF #2 1.04

- ELF #2 is better than ELF#1

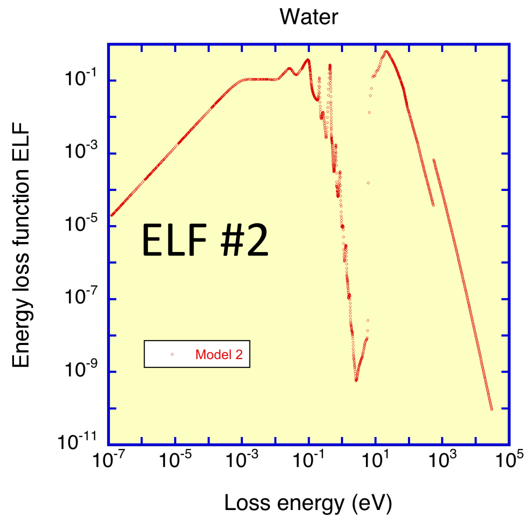

IMFP for water from ELF #2

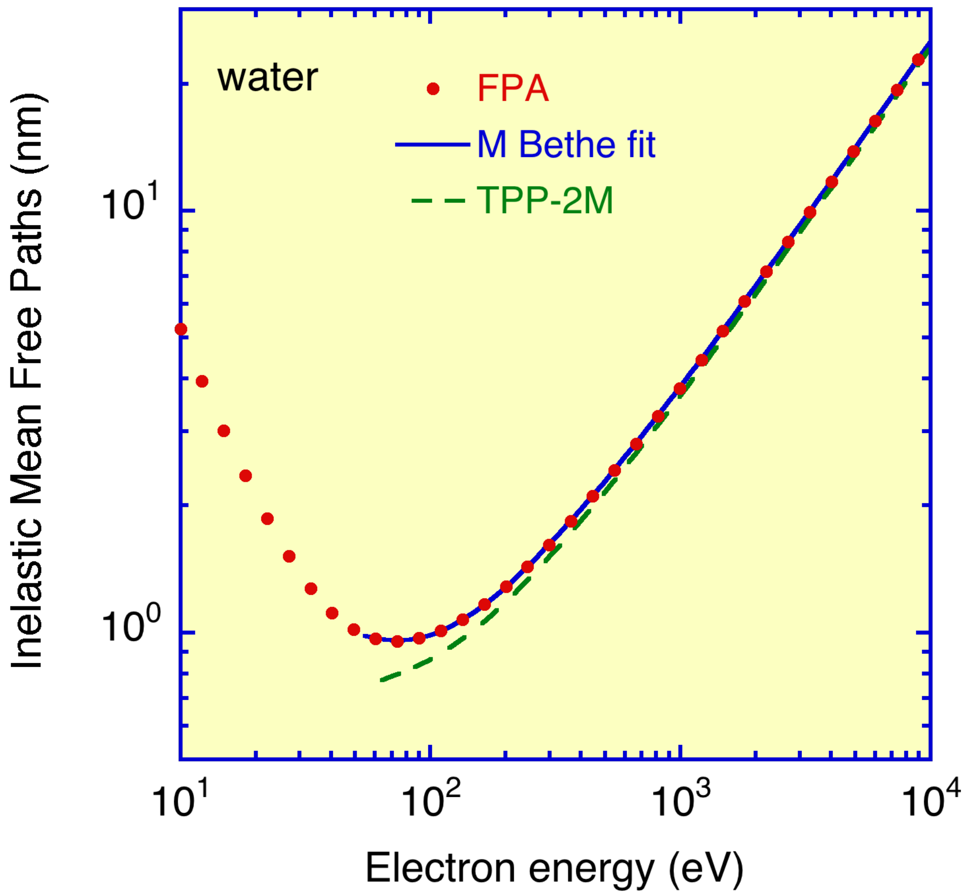

$$\lambda_S = \frac{\alpha(T)T}{E_p{}^2\left\{\beta_{nr}\left[\ln\left(\gamma_{nr}\alpha(T)T\right)\right] - C/T + D/T^2\right\}}$$

$$\beta_{nr} = -1.0 + 9.44/\left(E_p^2 + E_g^2\right)^{0.5} + 0.69\rho^{0.1} \; (\mathrm{eV^{-1}nm^{-1}})$$

$$\gamma_{nr} = 0.191\rho^{-0.5} \qquad (\mathrm{eV^{-1}})$$

$$C = 19.7 - 9.1U \qquad (\mathrm{nm^{-1}})$$

$$D = 534 - 208U \qquad (\mathrm{eVnm^{-1}})$$

$$U = \frac{N_v\rho}{M} = \left(E_p/28.816\right)^2$$

Fit with rel. M. Bethe eq. : RMS 0.1%
(50eV – 30 keV)

>200 eV : IMFPs of TPP-2M
good agreement (RMS 4.5%)

4. Analysis of IMFPs

Comparison : FPA, SPA and SSPA; q-dependence of ELF

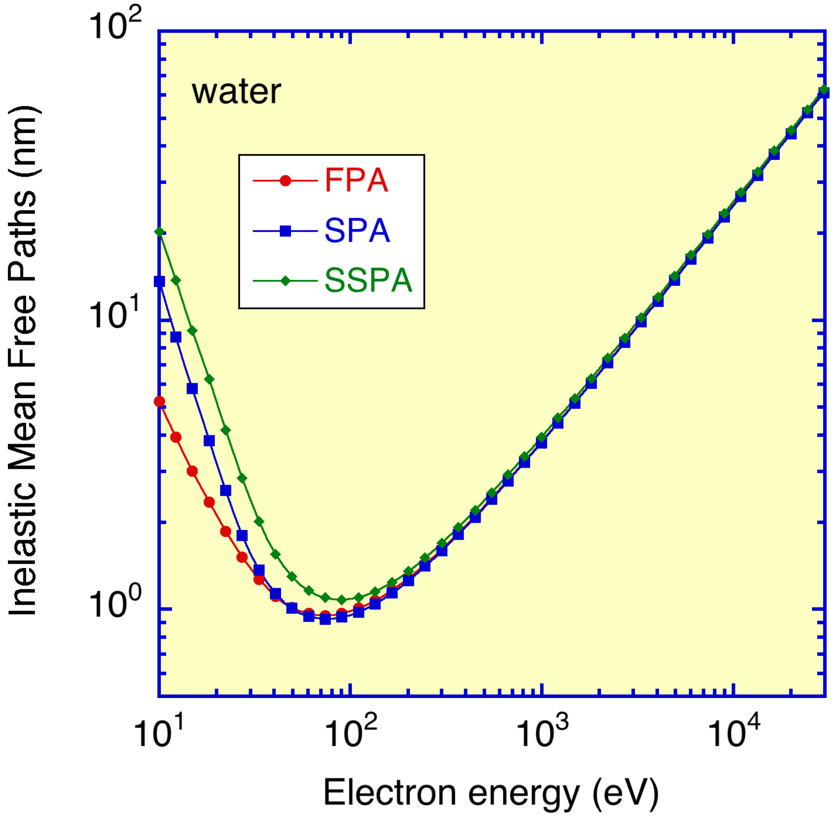

Used optical ELF(w,q=0) : same
q-dependence : different ELF (w, q>0)

Low energy region < 200 eV

- depends on dispersion equation for q>0

Under 40 eV (FPA – SPA)

- depend on single electron exaction

FPA :

$$\mathrm{Im}\left[\frac{-1}{\varepsilon(q,\omega)}\right] = \mathrm{Im}\left[\frac{-1}{\varepsilon(q,\omega)}\right]_{pl} + \mathrm{Im}\left[\frac{-1}{\varepsilon(q,\omega)}\right]_{se}$$

: FPA - smallest
: SPA - good agreement with FPA > 40 eV
: SSPA - largest over 10 eV – 30 keV

- mainly due to q-dependence of ELF

Over 300 eV

- Good agreement among FPA, SPA and SSPA

4. Analysis of IMFPs

Comparison : FPA, SPA and SSPA; q-dependence

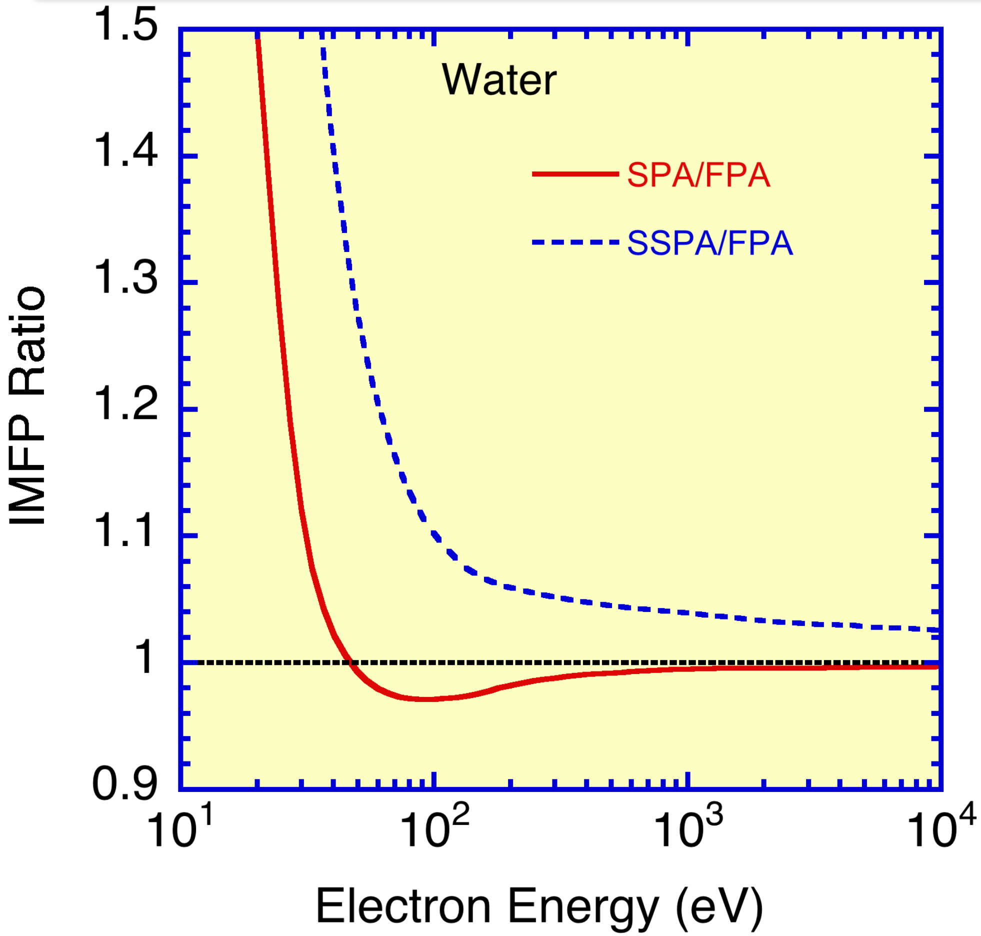

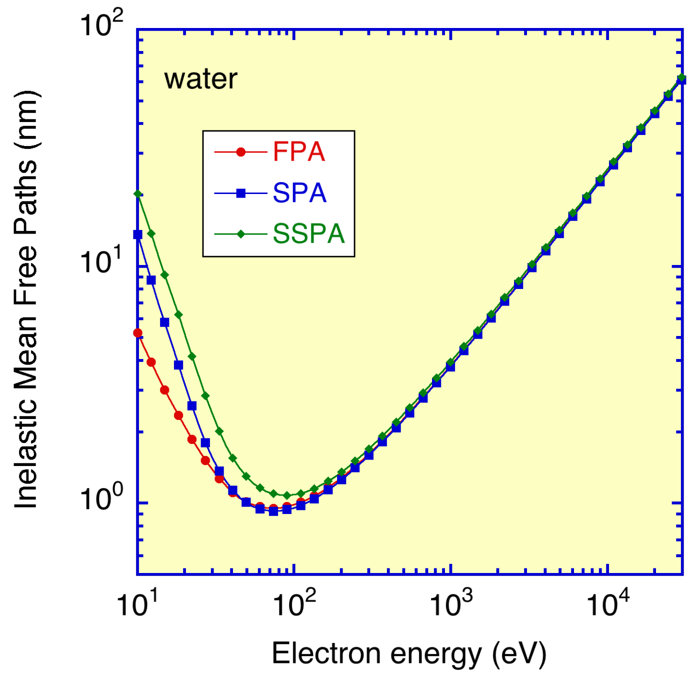

SPA $$\omega_q^2(\omega_p) = \omega_p^2 + \frac{1}{3}\left(k_F(\omega_p) q\right)^2 + \frac{q^4}{4}$$

SSPA $$\omega_q(\omega_p) = \omega_p + \frac{q^2}{2}.$$

Low energy region < 200 eV

- depends on dispersion equation for q>0

Under 40 eV (FPA – SPA)

- depend on single electron excitation

FPA :

$$\mathrm{Im}\left[\frac{-1}{\varepsilon(q,\omega)}\right] = \mathrm{Im}\left[\frac{-1}{\varepsilon(q,\omega)}\right]_{pl} + \mathrm{Im}\left[\frac{-1}{\varepsilon(q,\omega)}\right]_{se}$$

Analysis of IMFPs at high energy region with Fano plot

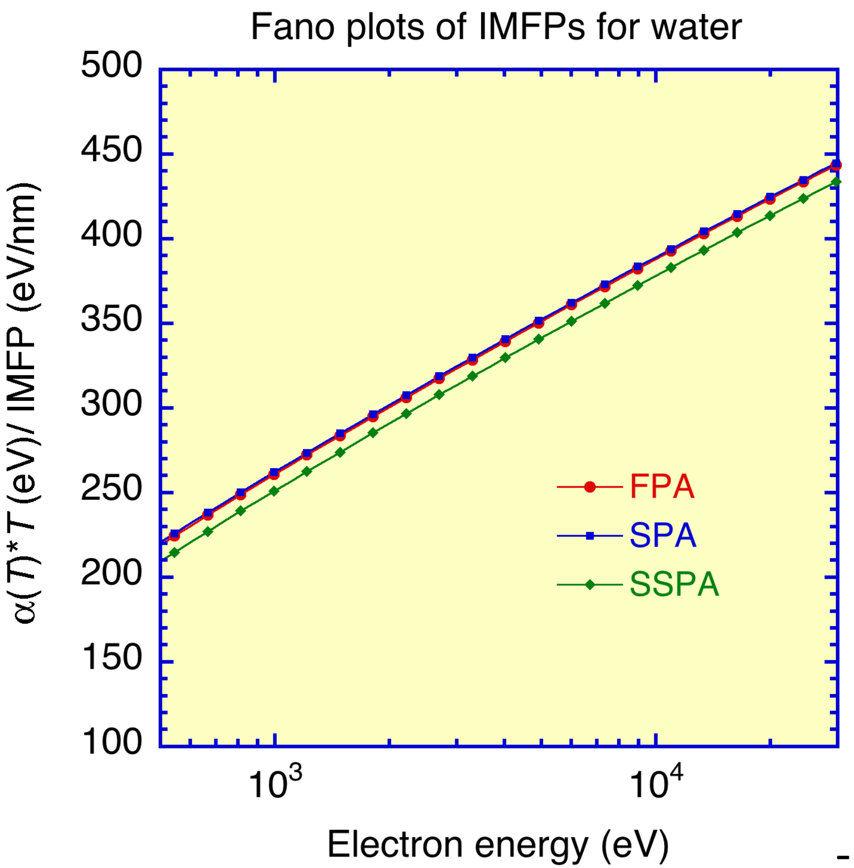

$$T/\lambda = E_p^2[\beta_{nr}\ln(\gamma_{nr}T)-(C/T)+(D/T^2)]$$

$$\approx E_p^2\beta_{nr}\ln(\gamma_{nr})+E_p^2\beta_{nr}\ln(T)$$

: total inelastic CS can be described by Bethe eq.

- Fano plot *T*/λ *vs.* ln (*T*) → straight line

$$E_p^2\beta_{opt} = E_p^2 M_{tot}^2/28.8N_v$$

$$M_{tot}^2 = \frac{2R\int_0^{\Delta E_{max}} \mathrm{Im}[-1/\varepsilon(\Delta E, q=0)]d(\Delta E)}{\pi\hbar^2\Omega_p^2}$$

- Slope : M_{tot}^2 (square of the dipole matrix element for all possible inelastic scattering processes)

- Intercept : function of q-dependence of ELF

α(T): conversion factor for relativistic correction

5. Comparisons with other calculations

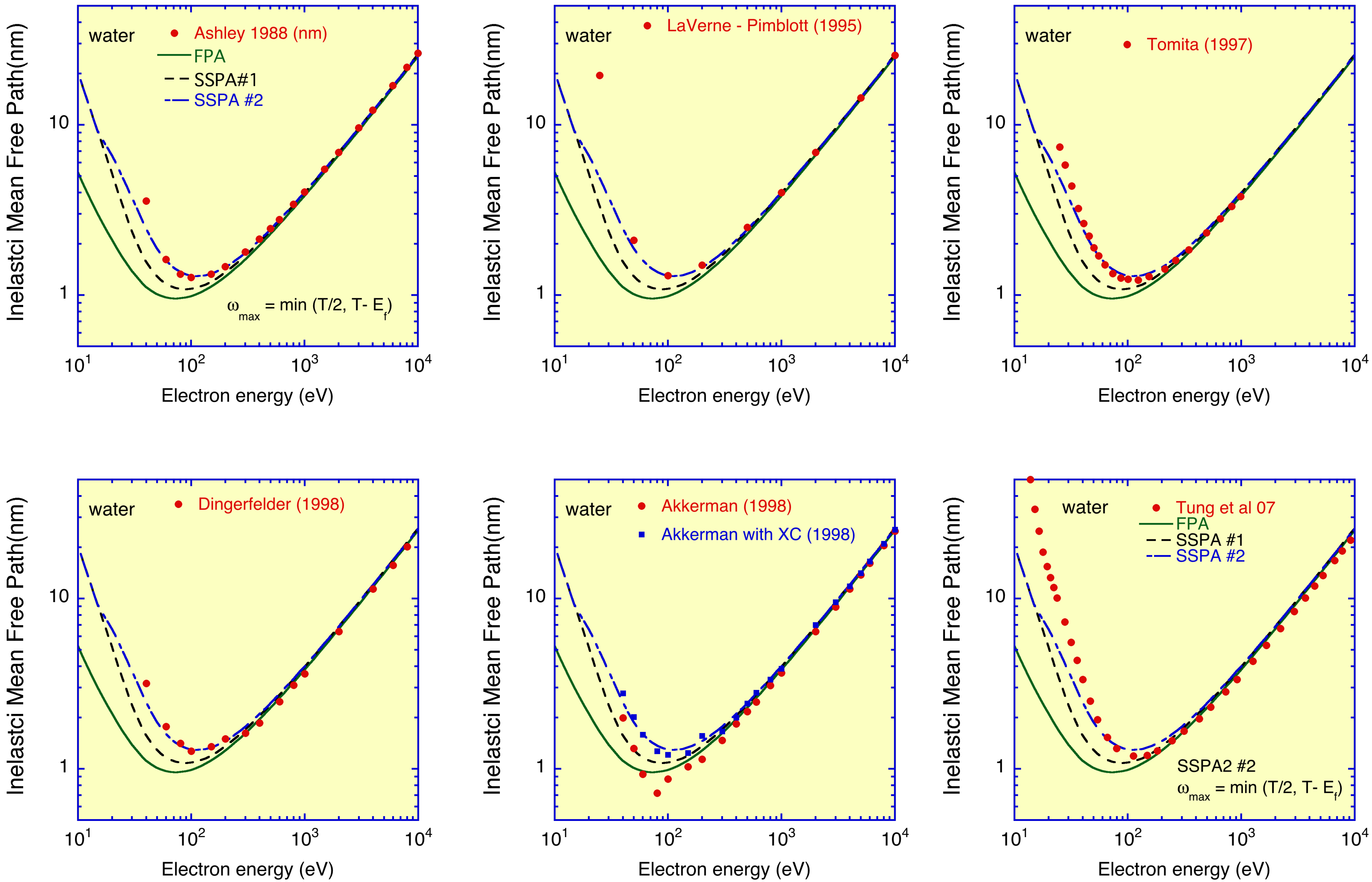

5. Comparisons with Emfietzoglou data

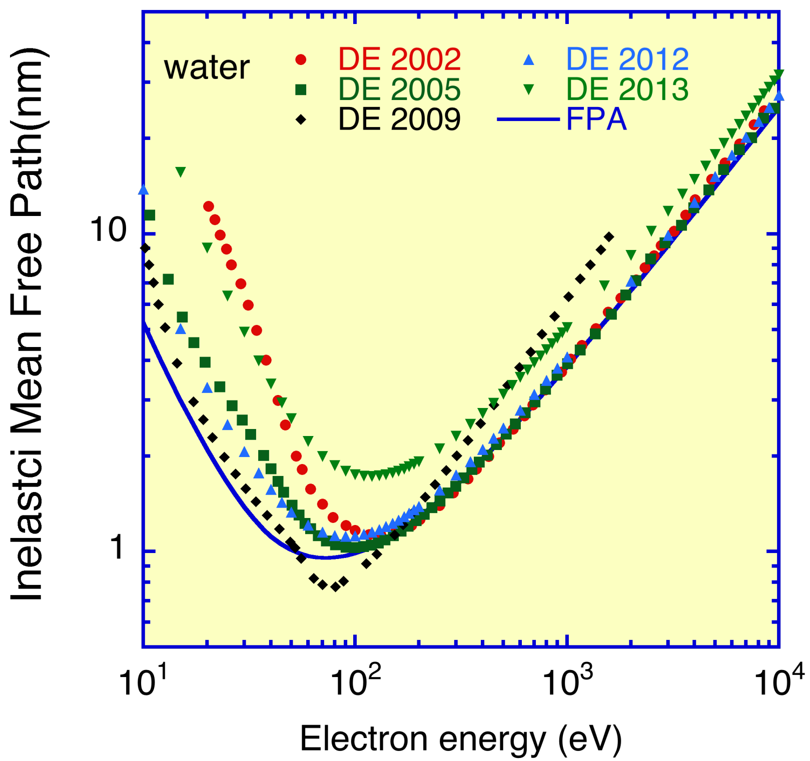

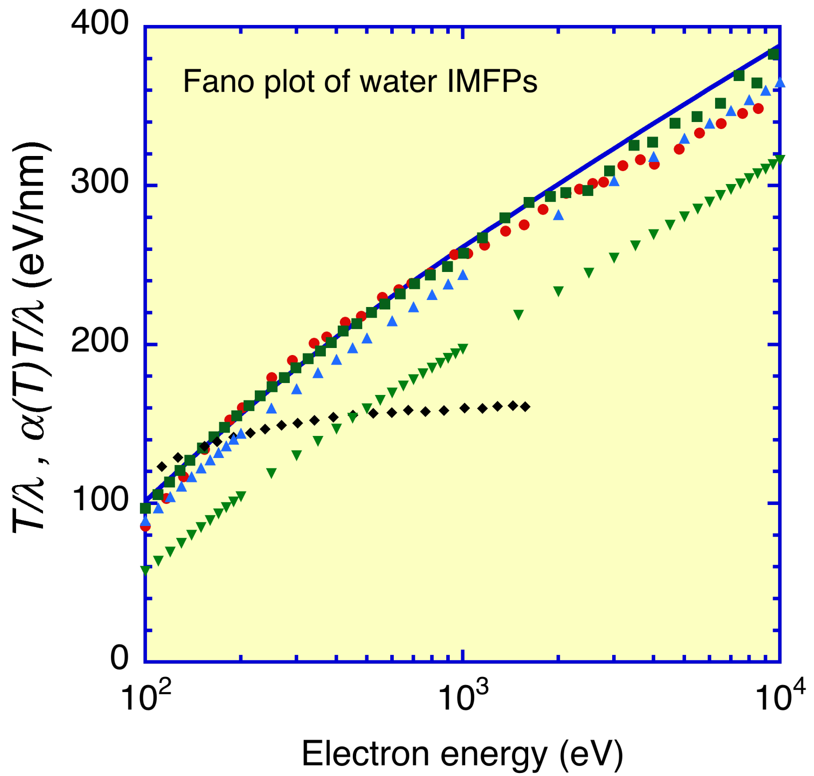

DE 2002 Heller optical data

DE 2009 Linhard + LFC (not ODM)

DE 05, 12, 13 : Hayashi optical data

$$T/\lambda = E_p^2[\beta_{nr}\ln(\gamma_{nr}T) - (C/T) + (D/T^2)]$$
$$\approx E_p^2\beta_{nr}\ln(\gamma_{nr}) + E_p^2\beta_{nr}\ln(T)$$

- Slope : $M_{tot}^2 \propto \mathrm{Im}[-1/\varepsilon(\Delta E, q=0)]$
- Intercept : function of q-dependence of ELF

5. Comparisons with Emfietzoglou data

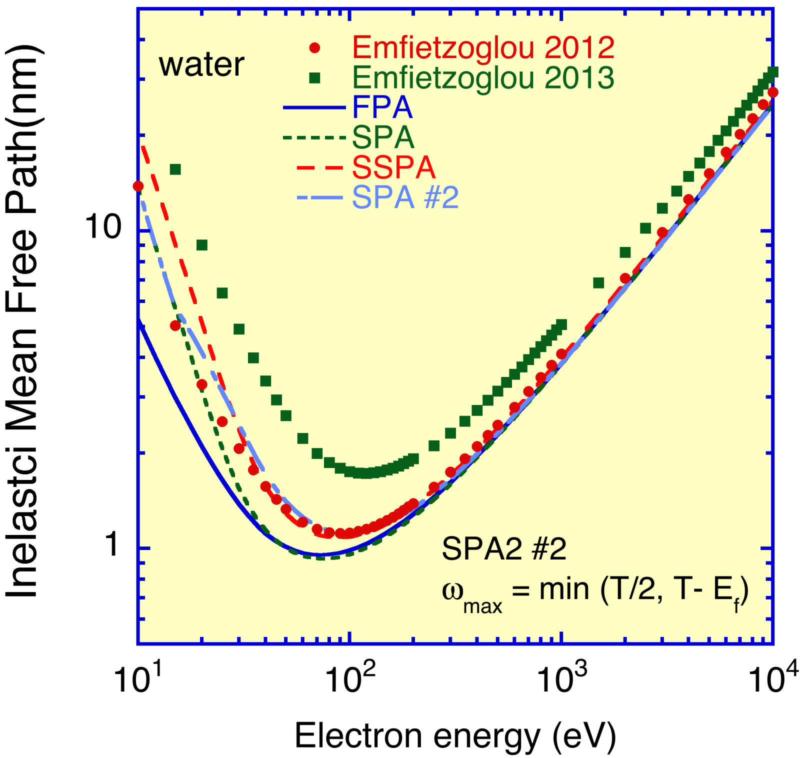

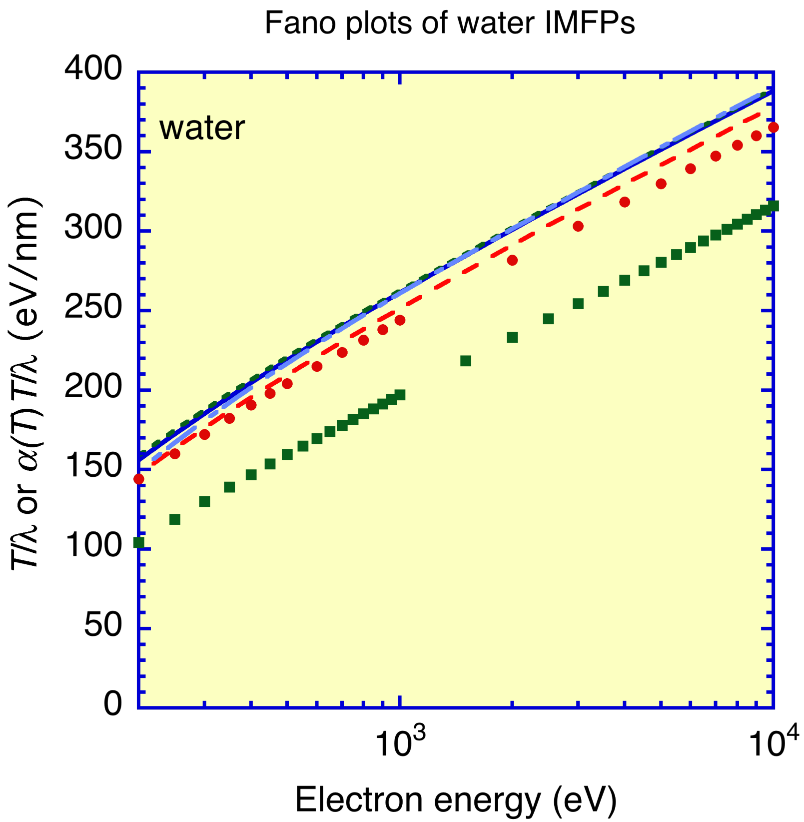

DE 12: ECN dispersion eq.

$$E_i(q) = E_i + g(q)\frac{q^2}{2m_e}$$

where $g(q) = 1 - \exp(-cq^d)$ and

$$\gamma_i(q) = \gamma_i + aq + bq^2$$

DE 13: XC including static and dynamic LFC

- Slope : $M_{tot}^2 \propto \mathrm{Im}[-1/\varepsilon(\Delta E, q=0)]$
- Intercept : function of q-dependence of ELF

Comparison : measured EALs

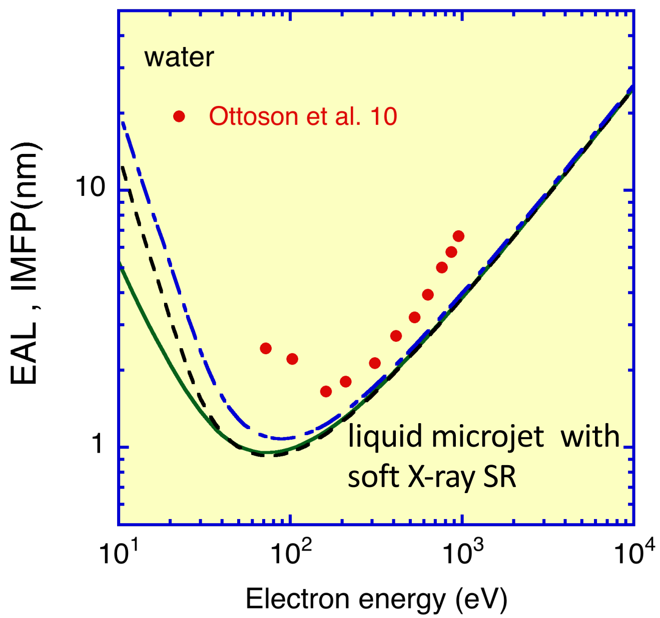

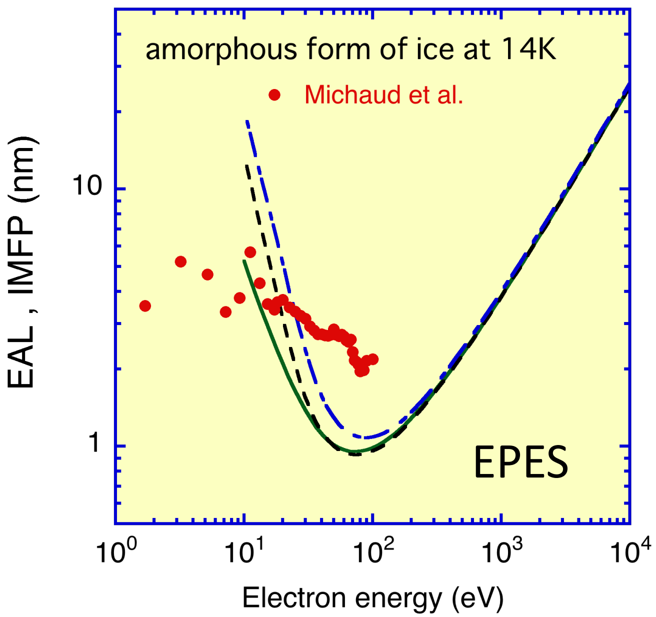

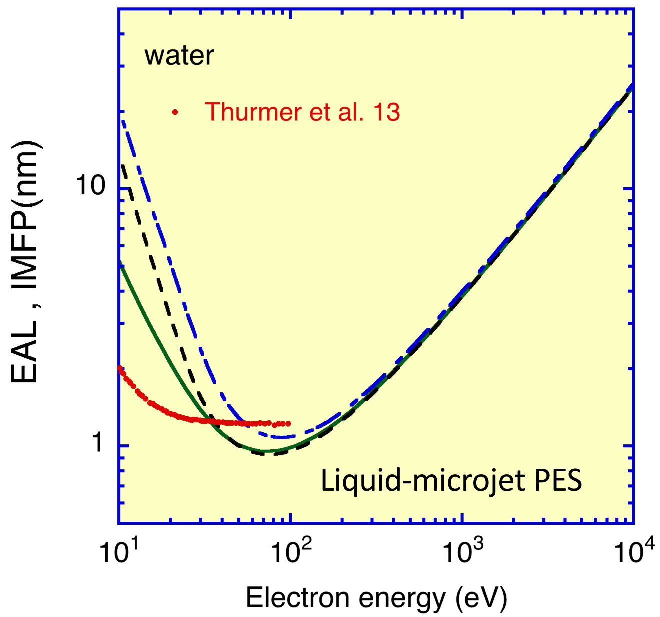

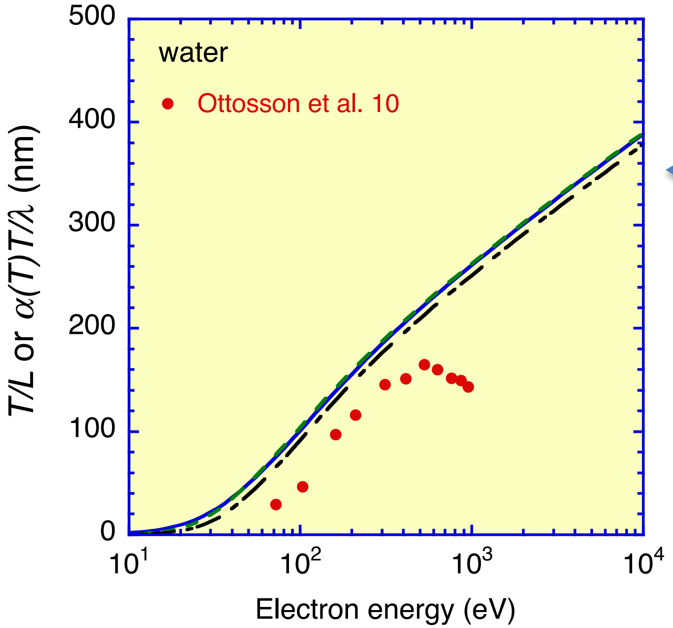

Fano plot

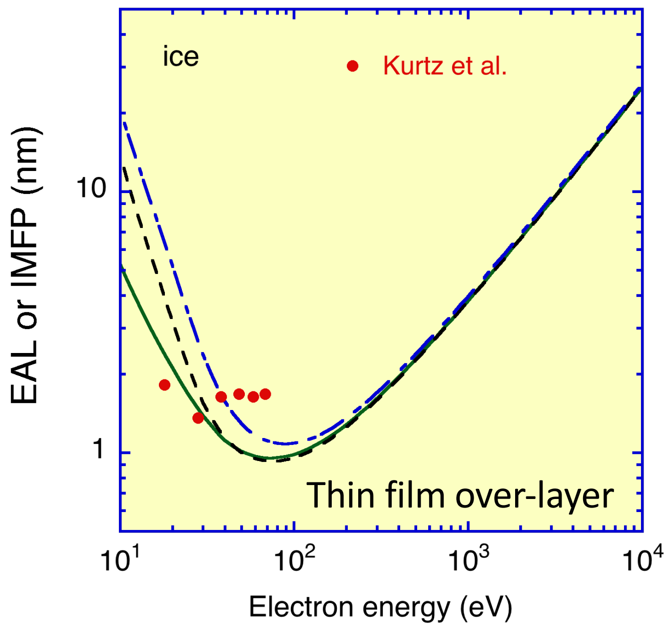

Summary

- We have calculated IMFPs of water from measured ELF using FPA. (10 eV – 30 keV)
- IMFPs were fitted by M. Bethe equation in the range of 50 eV – 30 keV using Fano plot (RMS differences: 0.1 %)
- IMFPs predicted by TPP-2M equation are in good agreement with IMFPs by FPA over 200 eV – 30 keV. (RMS: 4.5%)

- We compared our IMFPs with those of other calculations and experimental results
- We found

  : good agreement over 200 eV with majority of IMFP calculations (Ashley, Pimblott et al., Tomita et al., Dingerfelder et al. Akkerman et al., Emifietzoglou et al. (02, 05, 12), Tung et. al.)

  : our IMFPs are smallest among them under 200 eV (mainly due to algorithm (q-dependence on ELF model) and the maximum energy loss)

  : large differences between our IMFPs and IMFPs of Emifitzoglou (13) (due to XC correction)

Future work

- comparison with the IMFPs water calculated by Extended Mermin ELF model proposed by B. DA

- also estimate the effect electron exchange with Born-Ochkur correction

Thank you for your attention !